GENETICS

Changes in Copper Metabolism in Different Compartments of the Brain in Rats with Induced Fibrillogenesis

P. S. Babich, N. V. Tsymbalenko, O. O. Masalova, N. A. Platonova, M. M. Shavlovskii, L. V. Puchkova, and N. S. Sapronov

Translated from *Byulleten' Eksperimental'noi Biologii i Meditsiny,* Vol. 148, No. 8, pp. 184-190, August, 2009
Original article submitted October 30, 2008

Fibrillogenesis was induced in rats by injection of a fragment of neurotoxic protein, β-amyloid protein precursor, into the cerebral ventricle. Copper, iron, and zinc concentrations and relative activities of genes of copper-transporting protein and extracellular and intracellular cuproenzymes were evaluated in different brain compartments of these animals. Copper and zinc concentrations decreased significantly in different compartments of the brain of rats with experimental fibrillogenesis, while iron content did not change. According to the data of RT-PCR analysis, activities of genes of copper-transporting protein and extracellular coenzyme decreased. The expression of intracellular cuproenzyme genes and the content of SOD1 protein did not change, SOD1 activity in the cytosol decreased, and active SOD1 was detected in the mitochondrial intermembrane space. The relationship between fibrillogenesis and copper metabolism is discussed.

Key Words: *copper transporting protein and cuproenzyme genes expression; copper metabolism; fibrillogenesis*

Alzheimer's disease (AD) is a severe neurodegenerative disorder, developing as a result of formation of amyloidogenic β-peptide (Aβ) from β-amyloid protein precursor (APP). The main morphological sign of AD are extracellular plaques containing Aβ fibrils with abnormal conformation [13]. The biochemical marker of the disease is hyperphosphorylation of tau-proteins, whose location changes during AD development, which leads to their appearance in the cerebrospinal fluid. Among the hypothetical causes leading to AD development are genetic factors, slow viral infections, oxidative stress, and alimentary deficiency of copper or disorders in its metabolism [2,8]. However, the real etiology of AD remains unknown, and there is still no effective therapy for this condition. The development of approaches to AD treatment is carried out on APP transgenic mice [16]. Rats with Alzheimer's type dementia (ATD) induced by injection of neurotoxic synthetic fragment of Aβ into the brain ventricles are also used as the model [14]. We think that this model has certain advantages. First, ATD is caused without intervention into the genome, all the consequences of this intervention are in fact neglected and only hyperexpression of APP gene is taken into consideration. Second, copper metabolism, disorders in which are presumably associated with AD development, differs significantly in mice and humans, while in rats and humans it is virtually the same [3].

We studied the distribution of copper, iron, and zinc and the expression of genes of proteins involved

Institute of Experimental Medicine, Russian Academy of Medical Sciences, St. Petersburg, Russia. ***Address for correspondence:*** puchkovalv@yandex.ru. L. V. Puchkova

in copper metabolism in various brain structures of rats with ATD. Activities of genes encoding high-affinity importer of copper (CTR1 protein) and two copper transport ATPases (ATP7A and ATP7B) were analyzed. The function of ATP7A in the brain hypothetically consists in absorption of copper ions and their incorporation into cuproenzymes synthesized in the secretory pathway of the cell. The function of ATP7B consists in elimination of copper and its incorporation into ceruloplasmin (CP) in cisterns of the Golgi complex [10]. In addition, we studied activity of the gene encoding CP, polyfunctional multicopper blue oxidase [15]. Ceruloplasmin is a universal copper donor for nonhepatocytic cells and a ferroxidase regulating the two-way transport of iron ions. Two mRNA are formed from the primary transcription product of this gene as a result of alternative splicing: mRNA encoding secretory CP (realizes copper transport and iron import) and mRNA encoding CP bound to the plasma membrane through glycosylphosphatidyl inositol anchor (GPI-CP; involved in iron export). Hence, CP gene is regarded as a gene encoding universal donor of copper for nonhepatocyte cells (secretory CP) and as a gene encoding two extracellular cuproenzymes (CP and GPI-CP). In addition to copper metabolism genes, we studied the expression of the genes encoding APP and two cuproenzymes. We studied the expression of APP gene, because this protein is hypothetically involved in copper transport to cells by reducing Cu(II) to Cu(I) [12]. This reaction is the key step in copper import into the cell, because CP delivers oxidized copper ions Cu(II) to the cell, while CTRI binds only Cu(I). The genes encoding intracellular cuproenzymes Cu/Zn superoxide dismutase (SOD1) and isoform 1 of cytochrome C-oxidase subunit IV (Cox4i1) are active in all cells. Hence, the set of studied genes constitutes virtually the complete chain of copper transport to its incorporation in cuproenzymes.

MATERIALS AND METHODS

The study was carried out on female Wistar rats (180-200 g) from Rappolovo Breeding Center (Leningrad Region). The animals were kept 5-6 per cage under standard conditions on balanced rations with free access to water at 12:12 h day:night regimen and 60% humidity. Experimental animals were injected with 5 μl water suspension containing 15 μg aggregated peptide corresponding by sequence to β-amyloid neurotoxic peptide (^{10}YEVHHQKLVFFAEDV^{25}, Sigma) into the lateral cerebral ventricle to a depth of 3.8 mm through an operation hole made above the right lateral ventricle in coordinates A=0.8, L=-1.5 according to the rat brain atlas [6]. Controls were injected with 5 μl sterile bidistilled water. Experiments were carried out 21 days after surgery. The development of ATD was identified by the appearance of pronounced neuronal damage in histological preparations and by deceleration of food reflex conditioning [14]. After intracardial perfusion, the brain was removed and the needed tissue specimens were isolated according to the rat brain atlas [11]. Total RNA was isolated using TRIzol Reagent (TriPure Isolation Reagent, Gibco/Invitrogen) strictly according to the instruction. The resultant RNA preparations ($A_{260/280}$=1.9) contained no DNA admixtures or RNA degradation products according to electrophoresis in 1% agarose gel. The concentration of RNA was leveled by the content of 28S pRNA. The cytosol was isolated by differential centrifugation from tissue homogenate prepared in buffer containing 0.25 M sucrose, 40 mM Tris-HCl buffer (pH 7.4), 100 mM KCl, 5 mM $MgCl_2$, 5 mM dithiotreitol, and 1/1000 share of protease inhibitor mixture (Sigma). The mitochondrial intermembrane space (MIS) was obtained from the mitochondria isolated by differential centrifugation after preliminary exposure of the mitochondria to the "swelling—shrinking—freezing—defrosting" procedure as described previously [1]. Gene activities were evaluated by semiquantitative RT-PCR as described previously [1]. Densitometry of PCR products was carried out using Scion Image software. The results were expressed in arbitrary units as the proportion of the quantity of resultant PCR product on the given mRNA to the quantity of β-actin PCR product obtained on the same RNA preparations. The measurements on independent RNA preparations were carried out 3 times. The results differed by no more than 10%. Unique primers were selected by Gene Runner 3.0 software by the sequences of corresponding genes presented in the open data base (Table 1). Immunoblotting was carried out as described previously [1]. Electrophoresis of proteins was carried out in 10 or 8% PAAG under non-denaturing conditions or with 0.1% sodium dodecylsulfate as described previously [9]. Protein transfer from PAAG on nitrocellulose membrane (Hybond™ ECL™, Amersham Pharmacia Biotech UK Limited) was carried out by the semi-dry method on a Semi-Phor TE70 device (Hoefer Scientific Instruments). ECL Western Blotting Detection Reagent chemiluminescent detection system and Hyperfilm ECL X-ray film (Amersham), rabbit antibodies to glyceraldehyde-3-phosphate dehydrogenase (GD-3-PD) and to full-length recombinant SOD1 (Abcam) and second antibodies to rabbit γ-immunoglobulins conjugated with horseradish peroxidase (Amersham) were used. Activity of SOD1 in gel was evaluated using NBT as SOD1 competitor for H_2O_2: 30 μg protein was fractionated in 10% PAAG under non-denaturing conditions in the presence of 5 mM dithiotreitol. After electrophoresis, the gel (7×8×1 mm) was incu-

TABLE 1. Sequences of Primers Used for Detection of Mature Transcripts of Copper-Transporting Protein Genes

Gene		Primer sequence	Reaction conditions, product length
trivial	RGD nomenclature		
CP	*Cp*, No. 2387, NM_012532.1	f: agtaaacaaagtcacaacgaggaat	
		r: tcgtattccacttatcaccaattta	$t_{annealing}$ 57°C, 398 n. p.
GPI-CP	*Cp*, No. 2387, AF202115	f: agtaaacaaagtcacaacgaggaat	
		r: ctccttggtagatatttggaataaa	$t_{annealing}$ 57°C, 436 n. p.
CTR1	*Slc31a1*, No. 620059,	f: tgcctatgaccttctactttgg	
		r: atgaagatgagcatgaggaag	$t_{annealing}$ 57°C, 358 n. p.
ATP7A	*Atp7a,* No. 2179	f: gaagcctactttcccggctacaacagaagc	
		r: aggtacccaaggtttcagtgtccagctcc	$t_{annealing}$ 57°C, °421 n. p.
ATP7B	*Atp7b*, No. 2180	f: cagaagtactttcctagccctagcaagc	
		r: cccaccacagccagaaccttcctgag	$t_{annealing}$ 57°C, 332 n. p.
APP	*Apbal,* No. 620844	f: cctcgagaattacatcaccgcactg	
		r: ctccacagtggtcttcgtttcagtc	$t_{annealing}$ 57°C, 400 n. p.
SOD1	*Sod1*, No. 3731	f: acaatacacaaggctctaccactgcagg	
		r: tcatcttgtttctcgtggaccaccatag	$t_{annealing}$ 57°C, 220 n. p.
SOD2	*Sod2*, No. 24787	f: tccctgacctgccttacgactatgg	
		r: gcttgatagcctccagcaactctcc	$t_{annealing}$ 57°C, 285 n. p.
COX	*Cox4i1*, No. 68374	f: aagagagccatttctacttcggtgtg	
		r: caggctctcacttcttccattcattc	$t_{annealing}$ 57°C, 484 n. p.
b-actin	*Actb*, No. 81822	f: gaagatcctgaccgagcgtg	
		r: agcactgtgttggcatagag	$t_{annealing}$ 59°C, 360 n. p.

bated in 75 ml 1.23 mM NBT for 15 min. The gel was then rapidly washed in water and incubated in 75 ml 100 mM K-phosphate buffer (pH 7.0) with 28 mM TEMED in the darkness for 15 min, after which riboflavin was added to a final concentration of 28 μM and incubation was continued for 15 min longer. In order to initiate photochemical reaction, the gel was exposed to UV light. After several minutes colorless zones appeared in SOD1-containing sites against the background of dark-blue gel. The metal concentrations were evaluated by atomic absorption spectrometry with electrothermal atomization and Zeeman correction of nonselective absorption on a Perkin Elmer 4100ZL spectrometer with end-capped THGA analyzer, Pd-Mg modifier (3 μg Pd and 9 μg Mg per sample) with automated delivery of samples; the measurements were carried out 3 times in each sample. The samples were prepared as described previously [1]. Tissue samples ≤100 mg were collected for measurements of metal concentrations. Metal ion solutions (Spectolab A/S) served as the reference samples. The results were expressed in μg/g wet tissue. The data are presented as mean±square deviation (n=5); the differences between the compared parameters were evaluated using Student's t test (p<0.05).

RESULTS

Seven anatomically well-discernible brain compartments were evaluated: cortex, cerebellum, hippocampus, amygdala, pituitary, hypothalamus, and vascular plexus. Of these, only the vascular plexus is not a nervous tissue formation; it is formed by ependymal cells and takes an active part in the maintenance of copper balance in the brain. The rest compartments are formed mainly by the nervous tissue cells. We previously showed that they differ by specific content of copper, combinations of copper-transporting protein genes expressed in then, quasistationary concentration of mRNA encoding these proteins, and intracellular distribution of their immunoreactive polypeptides [1]. In experimental series I, the concentrations of copper, iron, and zinc were measured in the samples prepared from brain compartments collected from 5

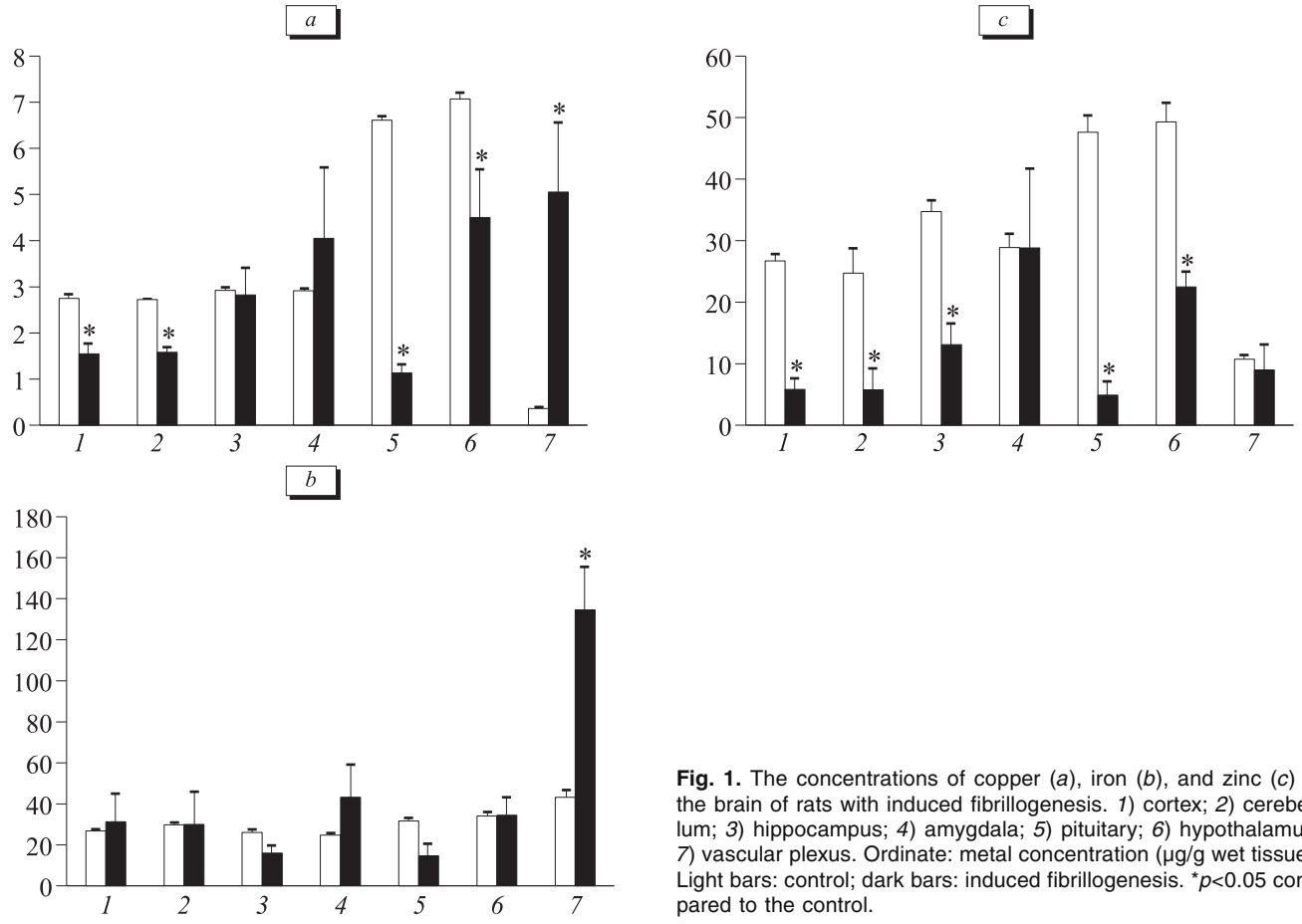

Fig. 1. The concentrations of copper (*a*), iron (*b*), and zinc (*c*) in the brain of rats with induced fibrillogenesis. *1*) cortex; *2*) cerebellum; *3*) hippocampus; *4*) amygdala; *5*) pituitary; *6*) hypothalamus; *7*) vascular plexus. Ordinate: metal concentration (μg/g wet tissue). Light bars: control; dark bars: induced fibrillogenesis. **p*<0.05 compared to the control.

rats (Fig. 1). The specific content of copper was significantly reduced in the cortex, cerebellum, pituitary, and hypothalamus of rats with ATD (Fig. 1, *a*). Copper concentrations in the amygdala and hippocampus were unchanged, while in the vascular plexus of these animals it increased almost 10-fold. Iron concentration changed (decreased significantly) only in the pituitary (Fig. 1, *b*). At the same time, iron concentration in the vascular plexus increased 4-fold. Zinc concentrations dropped several-fold in all brain compartments except the amygdala (Fig. 1, *c*) and did not change in the vascular plexus. These data indicate that induced fibrillogenesis caused a reduction of copper content in nervous tissue cells: in other words, this conditions simulated one of the main pathognomonic signs of AD [4]. However, alternative changes were observed in the ependyma. We failed to find published data on normal levels of copper, iron, and zinc in the vascular plexus. An interesting fact in our findings is a 3-fold lower concentration of zinc in the vascular plexus in comparison with the brain of control rats in general, this concentration being virtually the same as in the liver (10.7±0.7 and 11.8±0.7 μg/g wet tissue in the vascular plexus and liver, respectively). Normal iron concentration in the vascular plexus is higher than in brain compartments and is the same as in the liver (43.1±3.7 and 41.0±2.3 μg/g wet tissue in the vascular plexus and liver, respectively).

The expression of copper-transporting protein genes in rats with ATD is changed significantly (Fig. 2). No mRNA encoding CP, GPI-CP, ATP7A, and ATP7B were detected in our study in any of the studied brain compartments, including the vascular plexus (Fig. 2, *a-d*). Activities of CTR1 and APP genes were retained, but were significantly reduced (Fig. 2, *e*, *f*). The content of SOD1 gene mature transcripts was increased in the hippocampus and decreased in the hypothalamus (Fig. 2, *g*). The level of mRNA encoding Cox4i1 was reduced in the hippocampus (Fig. 2, *h*). Activities of Cox4i1 gene in the amygdala, pituitary, and hypothalamus were not measured. However, the decrease in the content of cuproenzyme mRNA, in contrast to mRNA of copper-transporting proteins (including CP and GPI-CP mRNA), was less significant in our model of AD. Interestingly, activities of CTR1, APP, SOD1, and Cox4i1 genes in the vascular plexus cells did not change. Presumably, this can be explained by the mesenchymal origin of this brain compartment.

The relative content of SOD1 polypeptide and SOD1 activity of in the cytosol and MIS were mea-

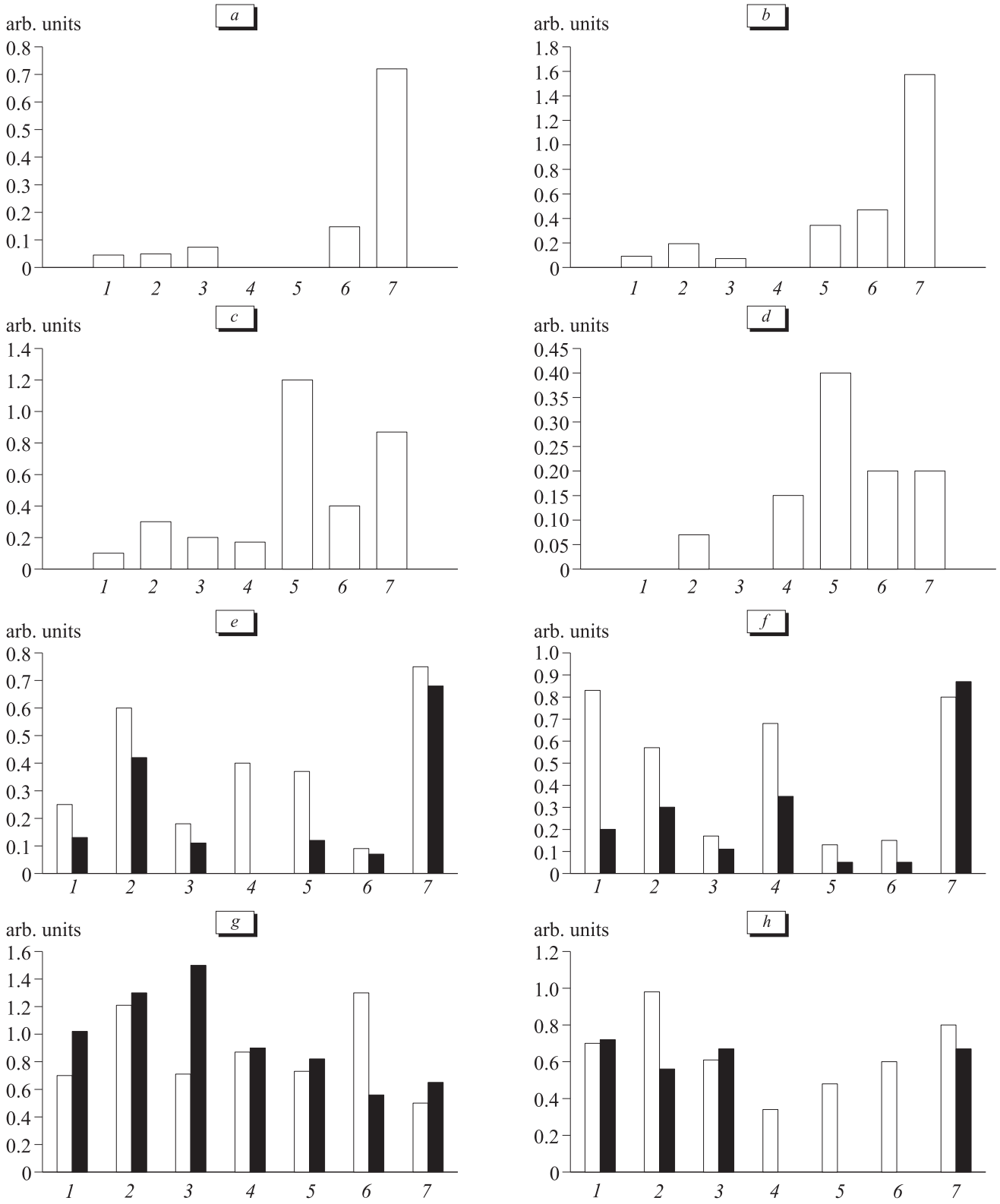

Fig. 2. Relative content of mRNA encoding copper-transporting proteins and cuproenzymes in the brain of rats with induced fibrillogenesis. *a-h*) content of PCR products obtained on mature mRNA by RT-PCR. *a*) secretory CP mRNA; *b*) GPI-CP mRNA; *c*) ATP7A mRNA; *d*) ATP7B mRNA; *e*) CTR1 mRNA; *f*) APP mRNA; *g*) SOD1 mRNA; *h*) Cox4i1 mRNA (no measurements were carried out in the amygdala, pituitary, and hypothalamus of rats with induced fibrillogenesis). Light bars: control group; dark bars: ATD model. *1*) cortex; *2*) cerebellum; *3*) hippocampus; *4*) amygdala; *5*) pituitary; *6*) hypothalamus; *7*) vascular plexus.

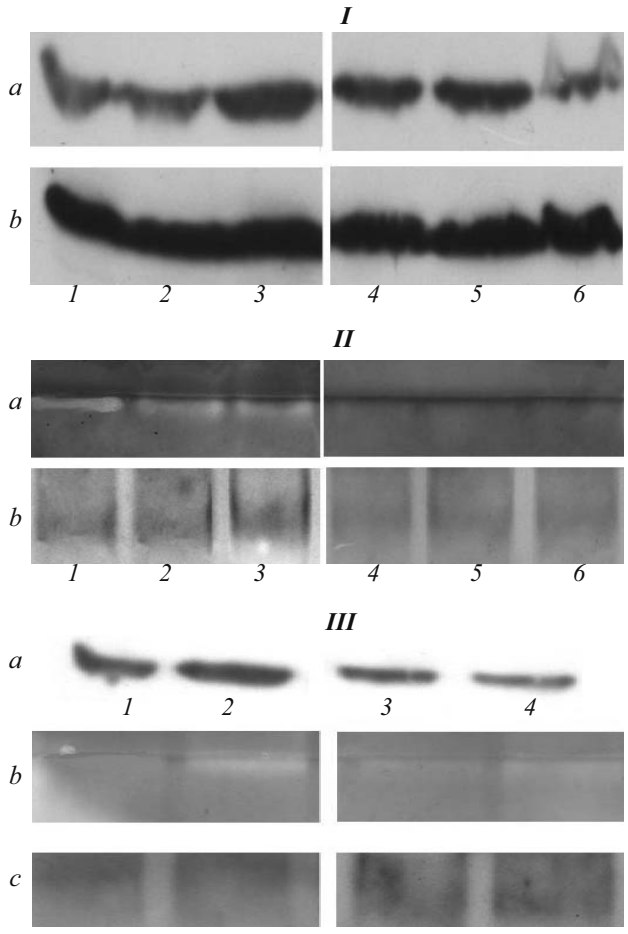

Fig. 3. Detection of SOD1 polypeptides in the cytosol and MIS. *I*, *II*) immunoblotting of cytosol isolated from the cortex (*1*), cerebellum (*2*), and hippocampus (*3*) of control rats and rats with induced fibrillogenesis (*4*, *5*, and *6*, respectively). *a*) antibodies to SOD1; *b*) antibodies to GD-3-PD. Electrophoresis was carried out in 10% PAAG with sodium dodecylsulfate. *II*: *a*) gel stained for SOD1 activity; *b*) immunoblotting with antibodies to SOD1 after electrophoresis in 10% PAAG under non-denaturing conditions. *III*: immunoblotting of intermembrane space isolated from the mitochondria of the cortex (*1* and *3*) and cerebellum (*2* and *4*) of control rats (*1* and *2*) and rats with induced fibrillogenesis (*3* and *4*). *a*) immunoblotting with antibodies to SOD1 after electrophoresis in 10% PAAG with sodium dodecylsulfate; *b*) SOD1 activity detected in gel after electrophoresis under non-denaturing conditions; *c*) immunoblotting with antibodies to SOD1 after electrophoresis in 10% PAAG under non-denaturing conditions.

sured in the cortex, cerebellum, and hippocampus (Fig. 3). In rats with ATD, SOD1 polypeptides are synthesized in all studied brain compartments (Fig. 3, *I*), but cytosolic activity of SOD1 in them is reduced in comparison with the control (Fig. 3, *II*). The content of SOD1 protein and activity of SOD1 were unchanged in MIS isolated from the cortical and cerebellar cells of rats with ATD (Fig. 3, *III*).

These data indicate that the concentrations of copper and zinc decreased in the brain of rats with ATD similarly as in patients with AD [5]. This results from competitive binding of copper ions on the cell membrane and/or in the cerebrospinal fluid by the injected neurotoxic peptide, which prevents their penetration into the cell. In the copper/peptide complex, the metal induces the formation of hydroxyl radicals by the Fenton and Haber—Weiss type reactions [7]. This disturbs spatial arrangement of the peptide and leads to the formation of aggregations impairing the Cu(II)→Cu(I) transformation catalyzed by APP. These changes result in a decrease of copper content in the cells. Our findings suggest that our model of ATD is adequate for the development of approaches to AD treatment.

The study was supported by the Russian Foundation for Basic Research (grants No. 06-04-49786 and No. 09-04-01406).

REFERENCES

1. N. A. Platonova, S. V. Barabanova, R. G. Povalikhin, *et al.*, *Izv. Rossiisk. Akad. Nauk*, Ser. *Biology*, No. 2, 108-120 (2005).
2. P. Adlard and A. I. Bush, *J. Alzheimer's Dis.*, **10**, Nos. 2-3, 145-163 (2006).
3. A. Cabrera, E. Alonzo, E. Sauble, *et al.*, *Biometals*, **21**, No. 5, 525-543 (2008).
4. M. A. Cater, K. T. McInnes, Q. X. Li, *et al.*, *Biochem. J.*, **412**, No. 1, 141-152 (2008).
5. M. A. Deibel, W. D. Ehmann, and W. R. Markesbery, *J. Neurol. Sci.*, **143**, Nos. 1-2, 137-142 (1996).
6. E. Fifkova and J. Marsala, *Stereotaxic Atlas for the Cat, Rabbit, and Rat*, Praha (1960).
7. E. Gaggelli, H. Kozlowski, D. Valensin, and G. Valensin, *Chem. Rev.*, **106**, No. 6, 1995-2044 (2006).
8. L. M. Klevay, *Med. Hypotheses*, **70**, No. 4, 802-807 (2008).
9. U. K. Laemmli, *Nature*, **227**, No. 5259, 680-685 (1970).
10. S. Lutsenko, N. L. Barnes, M. Y. Bartee, and O. Y. Dmitriev, *Physiol. Rev.*, **87**, No. 3, 1011-1046 (2007).
11. A. Mitro and M. Palkovits, *Morphology of the Rat Brain Ventricles, Ependyma, and Periventricular Structures*, Budapest (1981).
12. C. Opazo, M. I. Barria, F. H. Ruiz, and N. C. Inestrosa, *Biometals*, **16**, 91-98 (2003).
13. G. W. Small, *Kaplan and Sadock's Comprehensive Textbook of Psychiatry*, Eds. B. J. Sadock, V. A. Sadock, Philadelphis (2005).
14. I. I. Stepanov, N. N. Kuznetsova, B. I. Klement'ev, and N. S. Sapronov, *Neurosci. Behav. Physiol.*, **37**, No. 6, 583-590 (2007).
15. V. Vassiliev, Z. L. Harris, and P. Zatta, *Brain Res. Brain Res. Rev.*, **49**, No. 3, 633-640 (2005).
16. Y. Yoshiike, T. Kimura, S. Yamashita, *et al.*, *PLoS One*, **3**, No. 8, e3029 (2008).